International Food Research Journal 30(3): 709 - 722 (June 2023)
Journal homepage: *http://www.ifrj.upm.edu.my*

Response surface optimisation of technological parameters for producing *Ganoderma lucidum* by solid-state fermentation from *Panax notoginseng* residues and kinetics

*Tan, X., *Chen, F., Hu, W., Guo, J. and Yang, Y.

College of Resources and Environment,
Chengdu University of Information Technology, Chengdu 610225, China

Article history

Received:
28 June 2022
Received in revised form:
24 October 2022
Accepted:
9 December 2022

Keywords

solid-state fermentation,
Ganoderma lucidum,
response surface optimisation,
kinetics,
Panax notoginseng residues

Abstract

The present work aimed to investigate the optimal control strategy for *Ganoderma lucidum* (Chuanzhi No. 6) fermentation from *Panax notoginseng* residue. Optimisation of the solid-state fermentation (SSF) technical parameters, including inoculum dosage, fermentation temperature, and fermentation time was carried out using the single-factor and Box-Behnken design methods. Results showed that the optimal technical parameters were inoculum dosage of 15.28%, fermentation temperature of 28.42°C, and fermentation time of 14 d. The predicted maximum biomass of *G. lucidum* was 0.4327 g, which was also verified by validation experiments. The biomass of *G. lucidum* increased significantly with optimised technological parameters. The logistic equation, the Boltzmann function, and the four-parameter logistic equation were respectively suitable for modelling *G. lucidum* growth kinetics (R^2 = 0.9754), *Ganoderma* triterpene production kinetics (R^2 = 0.9897), and the matrix consumption kinetics (R^2 = 0.9826). These models can be used to predict the SSF process of *G. lucidum*, thus providing a theoretical basis for the development of new *G. lucidum* drugs, while at the same time recycle *Panax notoginseng* residue.

DOI
https://doi.org/10.47836/ifrj.30.3.14

Introduction

Ganoderma lucidum is a traditional mushroom with high medicinal value in China. Over the past 2,000 years, its medicinal value has been recognised (Dan *et al.*, 2016). The main active ingredients of *G. lucidum* and their medicinal effects have been studied. *Ganoderma lucidum* has been reported to have anti-tumour (Dan *et al.*, 2016) and anti-inflammatory effects (Akihisa *et al.*, 2007; Ko *et al.*, 2008; Gandia *et al.*, 2021; Berovic *et al.*, 2022), immune regulation (Fazenda *et al.*, 2010; Zhao *et al.*, 2018), antineurasthenia (Mahapatra and Banerjee, 2013), liver protection (Mowsumi *et al.*, 2013; Jang *et al.*, 2014), analgesic (Lam *et al.*, 2008), and anti-human immunodeficiency virus (HIV)-1 and HIV-1 protease activities. To date, more than 300 active substances have been successfully separated and purified from *G. lucidum* (Lam *et al.*, 2008; Wu *et al.*, 2013), including polypeptides, polysaccharides, *Ganoderma* triterpenes, amino acids, fatty acids, trace elements, and organic acids (Boh *et al.*, 2007). Among these substances, polysaccharides and *Ganoderma* triterpenes are the most important active ingredients (Tang *et al.*, 2009; Liu *et al.*, 2010), and have been used to study cancer suppression and anti-inflammatory effects (Huie and Di, 2004).

With the rapid development of the Chinese traditional medicine industry in China, the discharge of Chinese medicine residues is increasing, and currently exceeds 70 million tons per year (Yuan *et al.*, 2020). Chinese medicine residue contains proteins, starches, celluloses, amino acids, fatty acids, and trace elements that can be utilised by microorganisms, which have been proven to have added value. The treatment methods of traditional Chinese medicine residues mainly include incineration, landfill, and stacking, thus resulting in secondary pollution, waste of resources, and a large investment of funds. Li *et al.* (2019) studied the extraction of polysaccharides from *Panax notoginseng* residues and obtained 69.7% *P. notoginseng* polysaccharides, which improved the redevelopment and utilisation value of *P. notoginseng*

*Corresponding author.
Email: 329619195@qq.com ; cff1988@cuit.edu.cn

residues. Hsu *et al.* (2013) produced *G. lucidum* using American ginseng residue as a fermentation medium to verify the enrichment and transformation of the active substance ginsenosides, and found that the content of ginsenosides in the produced *G. lucidum* mycelial biomass was significantly increased. Chen *et al.* (2006) produced *G. lucidum* using traditional Chinese medicine residue as a medium, and found that the *G. lucidum* obtained had more active ingredients (polysaccharides and ganoderic acid). Gu *et al.* (2005) studied the two-way solid-state fermentation of 14 strains of *G. lucidum* and liquorice residue, and found that the polysaccharide content in the *G. lucidum* mycelial biomass greatly increased. Hu *et al.* (2002) found that the control of capillary water in the fermentation process of *G. lucidum* is the key to improving its yield. An *et al.* (2021) conducted solid-state fermentation (SSF) on different agricultural and forestry residues, and found that different types of fungi have preferences for agricultural and forestry residues, and cottonseed husks and corncobs can help increase *G. lucidum* production.

Using traditional Chinese medicine residues as a solid fermentation medium to produce *G. lucidum* can reuse the nutrients and effective substances in the residues, and can also achieve bioenrichment and transformation to increase the content of active components in *G. lucidum*. It can not only turn waste into treasure, but also help solve the problem of environmental pollution.

In the present work, *G. lucidum* was produced by SSF from *P. notoginseng* residues. The technological parameters for the production of *G. lucidum* were optimised to increase its yield by Box-Behnken design. The kinetics of SSF was also studied by establishing a mathematical model to study the laws of SSF, including the laws of *G. lucidum* growth, matrix consumption, and product generation. The findings not only guide the scale-up design of fermentation reactors but also accurately control the fermentation process, thus providing theoretical guidance for the large-scale production of *G. lucidum* by SSF.

Materials and methods

Microorganism

Ganoderma lucidum (Chuanzhi No. 6, National Product Identification No. 2007045) was obtained from the Soil and Fertilizer Research Institute (SFRI, Sichuan Academy of Agricultural Sciences, China), and was cultivated on potato-dextrose agar (PDA) plates at 28°C. After 7-d incubation on PDA plates, *G. lucidum* strains were harvested.

Materials

Panax notoginseng residues were obtained from a Chinese patented medicine factory in Chengdu, and used after pre-treatments such as drying, crushing, and sieving.

Potatoes were purchased from the local farmers' market. Glucose, potassium dihydrogen phosphate (KH_2PO_4), magnesium sulphate ($MgSO_4$), trichloroacetic acid ($C_2HCl_3O_2$), sulphuric acid (H_2SO_4), anthrone ($C14_4H_{10}O$), sodium hydroxide (NaOH), vanillin ($C_8H_8O_3$), sodium potassium tartrate ($NaKC_4H_4O_6$), petroleum ether (60 - 90°C), sodium bisulphite ($NaHSO_3$), perchloric acid ($HClO_4$), ammonium sulphate ($(NH_4)_2SO_4$), acetic acid (CH_3COOH), sodium acetate (CH_3COONa), and ethanol (C_2H_6O) were of analytical reagents. Peptone, yeast extract powder, and agar were biochemical reagents. All reagents were purchased from Chengdu Chron Chemicals Co. Ltd.

Media

Potato dextrose agar (PDA)

The medium contained 1,000 mL potato extract, 20.0 g glucose, and 15.0 g agar. The medium was sterilised at 121°C for 20 min, and used for the cultivation of *G. lucidum* strains.

Seed culture

The medium contained 20.0 g potatoes, 2.0 g glucose, 0.2 g peptone, 0.1 g KH_2PO_4, 0.06 g $MgSO_4$, 0.3 g yeast powder, and 100 mL distilled water, which was used to prepare *G. lucidum* seed culture.

Comprehensive medium

The medium contained 20 g potatoes, 2.0 g glucose, 0.2 g peptone, 0.1 g KH_2PO_4, 0.06 g $MgSO_4$, 2.0 g agar powder, 0.3 g yeast powder, and 100 mL distilled water, which was used for the expansion and storage of *G. lucidum*.

Solid-state fermentation medium

The medium contained 10.00 g *P. notoginseng* residues, 5.47% yeast powder, and 0.31% KH_2PO_4. The initial water content of the medium was 67.71%, and the pH was neutral. The medium was sterilised at

121°C for 1.0 h, and used for the response surface optimisation experiment of SSF technological parameters and the kinetics experiment of *G. lucidum* growth.

Experimental method

Pre-treatment of Panax notoginseng residues

The wet *P. notoginseng* residues were air-dried naturally, and then oven-dried at 60°C for 72 h. After crushing and sieving (60 mesh), they were placed in a desiccator.

Seed culture

The preparation of seed culture began by transferring 0.5 cm^2 of *G. lucidum* mycelial plug obtained from the PDA into a 100 mL seed culture medium, and cultivating in a 250 mL conical flask. The medium was incubated in a constant temperature water bath shaker at 28°C and 150 rpm for 4 d.

Preparation of pure mycelium

Pure mycelium was prepared in the same way as the seed culture. *G. lucidum* pure mycelium obtained after fermentation was filtered through eight layers of gauze, and washed with distilled water to remove residual nutrients. The filtered mycelium was oven-dried at 65°C, and used for the standard curve determination of *G. lucidum* mycelial biomass.

Optimisation experiment of technology parameters by SSF

The Box-Behnken design (BBD) was used to optimise the technical parameters for producing *G. lucidum* by SSF. Based on the single-factor experiments, a three-factor three-level BBD experimental plan with seventeen points (five central points) was carried out to determine the inoculum (X_1), fermentation temperature (X_2), and fermentation time (X_3) for the maximum mycelial biomass of *G. lucidum* (Y). The variables and code levels of the BBD experimental plan are given in Table 1. The response surface design and experimental results for *G. lucidum* mycelial biomass are given in Table 2. The experimental results were analysed with the coefficient of determination (R^2) and analysis of variance (ANOVA) obtained by Design-Expert 8.0 software (Stat-Ease, Inc.). The high-line plot and the three-dimensional response surface were obtained by keeping one independent variable constant, and changing the levels of the other variables.

Kinetics experiment of solid-state fermentation

The *Ganoderma lucidum* seed liquid with 15.2% (v/w) inoculum was inoculated on SSF medium, which was sterilised at 121°C for 1 h, and the medium was cultured under the optimal conditions obtained by the response surface experiment in a constant temperature and humidity biochemical incubator (Shaoguan Keli EI Co, Ltd., China). From day 0, ten conical flasks were removed every day to determine the mycelial biomass of *G. lucidum*, the total sugar content, and the *Ganoderma* triterpene content. All values were averaged from three parallel experiments.

Measurement of Ganoderma lucidum mycelial biomass

The nucleic acid extraction method was used to indirectly measure the *G. lucidum* mycelial biomass. The OD_{260} value of the nucleic acid extract was measured by ultraviolet spectrophotometry.

Measurement of Ganoderma lucidum polysaccharides

Fifteen millilitres of 75% ethanol was added to 0.05 g of starch-removed *G. lucidum* mycelial biomass (Nie *et al.*, 2013), which was then alcohol-extracted in a 60°C water bath for 30 min to remove monosaccharides, oligosaccharides, and other substances. After centrifugation, the residue was transferred to 30 mL of distilled water, and extracted in a water bath at 80°C for 2 h. The extracted solution was added to 100 mL of distilled water and filtered. The content of *G. lucidum* polysaccharides in the filtrate was determined by the anthrone-sulphate method (Chinese Pharmacopoeia, 2015).

Measurement of Ganoderma triterpenes

Ganoderma triterpenes were determined by the method of Tsujikura *et al.* (1992). *G. lucidum* mycelial biomass (0.5 g) was washed with 25 mL petroleum ether to remove the oil contained in *G. lucidum*. The residue was washed with 30 mL of 95% ethanol into a 50 mL colorimetric tube, ultrasonically extracted for 30 min, and then centrifuged. The colorimetric tube containing 0.1 mL of supernatant was boiled to dry the solvent in a 100°C water bath, and then 0.2 mL of 5% vanillin solution and 0.8 mL of perchloric acid were added in sequence and mixed. The mixture was kept in a water bath at 60°C for 20 min. After cooling to room temperature, 5 mL of

Table 1. Factors and code levels of variables for the Box-Behnken design.

Variable	Unit	Code-level value	Factor value
Inoculum dosage (X_1)	%	-1,0,1	10,15,20
Fermentation temperature (X_2)	°C	-1,0,1	25,28,31
Fermentation time (X_3)	d	-1,0,1	10,12,14

Table 2. Response surface design and experiment results for *Ganoderma lucidum* mycelial biomass.

Number	X_1: Inoculum Dose (%)	X_2: Fermentation temperature (°C)	X_3: Fermentation time (d)	*Ganoderma lucidum* mycelial biomass (g)	
				Actual value	Predicted value
1	-1	-1	0	0.2611	0.2562
2	1	-1	0	0.2997	0.3008
3	-1	1	0	0.2810	0.2799
4	1	1	0	0.2982	0.3031
5	-1	0	-1	0.2499	0.2564
6	1	0	-1	0.3131	0.3136
7	-1	0	1	0.3855	0.3849
8	1	0	1	0.4021	0.3956
9	0	-1	-1	0.2688	0.2672
10	0	1	-1	0.2620	0.2565
11	0	-1	1	0.3432	0.3487
12	0	1	1	0.3838	0.3854
13	0	0	0	0.3918	0.3903
14	0	0	0	0.3871	0.3903
15	0	0	0	0.3955	0.3903
16	0	0	0	0.3865	0.3903
17	0	0	0	0.3865	0.3903

glacial acetic acid was added and mixed uniformly. The OD_{550} value was measured by visible spectrophotometry (Wang *et al.*, 2006).

Kinetics model

The kinetics model of the *G. lucidum* fermentation process included growth kinetics based on *G. lucidum* mycelial biomass, product generation kinetics based on *G. lucidum* triterpene production, and matrix consumption kinetics based on total sugar consumption.

Growth kinetics model

Monod and logistic equations are the most widely used to describe the growth kinetics models of microorganisms. The Monod equation is a theoretical model based on the following assumptions: (1) microbial growth is a balanced non-structural growth mode, and the cell composition only needs to be expressed by the parameter of the microbial concentration; (2) there is only one growth-restricting substrate in the medium, and other nutrients have little effect on the growth of the microorganisms; and (3) the model regards the growth of the microorganisms as a simple reaction, and assumes that the yield of the microorganism is constant. In the present work, SSF was carried out with *P. notoginseng* residues as the medium. The above conditions (2) and (3) were not in accord with the fermentation characteristics. There would be deviations if the Monod equation was used to describe the growth kinetics. The best model to

describe the growth of *G. lucidum* is the logistic equation (Gatto *et al.*, 1988; Qi and Wang, 1996):

$$\frac{dX}{dt} = \alpha X\left(1 - \frac{X}{X_m}\right) \quad \text{(Eq. 1)}$$

where, X and X_m = mycelial biomass at time t and the maximum biomass (g), respectively; t = fermentation time (d); and α = specific growth rate constant (h^{-1}).

The logistic model is a typical S-shaped curve, which can better reflect the effect of the quality increase of *G. lucidum* mycelial biomass during SSF on growth, and can better describe the growth law of *G. lucidum* mycelial biomass:

i. At the beginning of fermentation, the concentration of *G. lucidum* mycelial biomass X was much smaller than X_m, and the value of X/X_m can be ignored, $dX/dt = \alpha X$, which meant that the growth of *G. lucidum* mycelial biomass increased exponentially;
ii. After the logarithmic growth phase, the growth of *G. lucidum* mycelial biomass was in a stable growth period, $X = X_m$, then $dX/dt = 0$, which meant that the growth of *G. lucidum* mycelial biomass has stopped, $X = X_m$

We then integrate Eq. 1 with $t = 0$, $X = X_0$ as conditions:

$$X = \frac{X_m}{1+\left(\frac{X_m}{X_0}-1\right)e^{-\alpha t}} \quad \text{(Eq. 2)}$$

Product formation kinetics model

The change in *Ganoderma* triterpene production was composed of two maintenance stages with a very steep increase in between. The best model to describe the curve of fermentation change of *Ganoderma* triterpenes is Sigmoidal Boltzman's function (Hait *et al.*, 2002):

$$y = B_2 + \frac{B_1 - B_2}{1+e^{\frac{t-t_0}{a}}} \quad \text{(Eq. 3)}$$

where, y = production of *Ganoderma* triterpenes, %; t = fermentation time, d; B_1 = initial production of *Ganoderma* triterpenes, %; B_2 = final production of *Ganoderma* triterpenes, %; t_0 = abscissa value of the intersection point (inflection point) of the S curve and the centreline of the two asymptotes, d; and a = time constant, which was 1/4 of the ratio of the difference between the two asymptotes to the tangent slope of the S curve at the inflection point.

Matrix consumption kinetics model

A four-parameter logistic equation (Culpepper, 2016) was used to describe the curve of fermentation change of total sugar consumption in *P. notoginseng* residue substrate during the SSF:

$$R = D_0 + \frac{C - D_0}{1+\left(\frac{t}{t_{50\%}}\right)^{k_0}} \quad \text{(Eq. 4)}$$

where, R = total sugar content of *G. lucidum* mycelial biomass at time t, %; t = fermentation time, d; D_0 = total sugar content at the end of fermentation, %; C = total sugar content of *G. lucidum* mycelial biomass at the initial stage of fermentation, %; $t_{50\%}$ = time required for the total sugar content to decrease from C to D_0 when the distance was 50%, which can be regarded as the half-life based on D_0, d; and k_0 = dimensionless constant.

Results and discussion

Optimisation using the single-factor method

The effects of fermentation temperature (22 - 34°C), inoculation dosage (v/w, 1 - 30%), medium dose (7.5 - 17.5 g), and fermentation time (4 - 14 d) on *G. lucidum* mycelial biomass are given in Figure 1.

Fermentation temperature had a great influence on the growth of *G. lucidum*. The optimum temperature for *G. lucidum* growth in this system was 28°C, and its mycelial biomass reached the maximum value of 0.3569 g (Figure 1a). *G. lucidum* mycelial biomass had high metabolic rate at this temperature, and the metabolic enzyme activity produced by *G. lucidum* was also high. Hariharan and Nambisan (2013) found that *G. lucidum* produced the highest lignin-degrading enzyme activity at 27°C, which ensured the degradation and utilisation of substrates by it, and promoted its growth and reproduction, which was consistent with our research.

The inoculation dosage directly affects the growth cycle of microorganisms. Results obtained in the present work showed that *G. lucidum* mycelial biomass reached a higher level when the inoculation dosage was 15 - 20% (Figure 1b). When the inoculum was 1%, its mycelial biomass was low. This was due to the lower basal concentration of *G. lucidum*

mycelial biomass which slowed its growth and increased the lag period. When the inoculation dosage was greater than 20%, its mycelial biomass decreased rapidly. This might have been due to the excessive inoculum dosage caused the *G. lucidum* mycelial biomass to reproduce too quickly in the early stage of fermentation. A large number of metabolites played a feedback inhibitory effect on *G. lucidum* growth (Guan *et al.*, 2008), and then it entered the decay period early under the condition of limited nutrients.

The aeration of the fermentation medium is directly related to the medium dose. *G. lucidum* is an aerobic microorganism. The medium needs to have good aeration to ensure the oxygen supply for the growth of *G. lucidum*, and the dissipation of CO_2 and metabolic reaction heat during the fermentation process. When the medium dose was 7.5 - 10.0 g, the *G. lucidum* mycelial biomass was higher, and its change was not significant ($p > 0.05$) (Figure 1c). This was due to the good aeration performance of the medium which improved the efficiency of gas exchange, heat transfer, and mass transfer. When the medium dose was 10.0 - 15.0 g, its mycelial biomass decreased with increasing medium dose (Figure 1c). When the medium dose was greater than 15.0 g, *G. lucidum* mycelial biomass no longer decreased with increasing medium dose, and its change was not significant ($p > 0.05$). This was due to the excessive medium dose and the thick stacking of medium materials, thus resulting in poor aeration, mass inefficiency, and heat transfer. The temperature of the culture medium increased too quickly, *G. lucidum* could only grow on the medium surface, and the nutrients in the medium could not be fully utilised, which reduced its mycelial biomass, consistent with Yang *et al.* (2004). Therefore, the medium dose was determined to be 10.0 g from the perspective of product yield and quality.

The first six days of fermentation were the adaptation period, and *G. lucidum* mycelial biomass increased slowly with time, and then increased rapidly thereafter (Figure 1d). After 12 d fermentation, its biomass changed slightly. *G. lucidum* production cycle by SSF is generally long and easily infected with bacteria. However, too long a fermentation time can lead to a lack of nutrients in the medium, thus resulting in autolysis of the cell, a reduction in biomass, and an increase in production costs. Therefore, the fermentation time should be controlled within 12 - 14 d.

The results of the single-factor method showed that *G. lucidum* mycelial biomass reached a maximum level of 0.4074 g after 14 d.

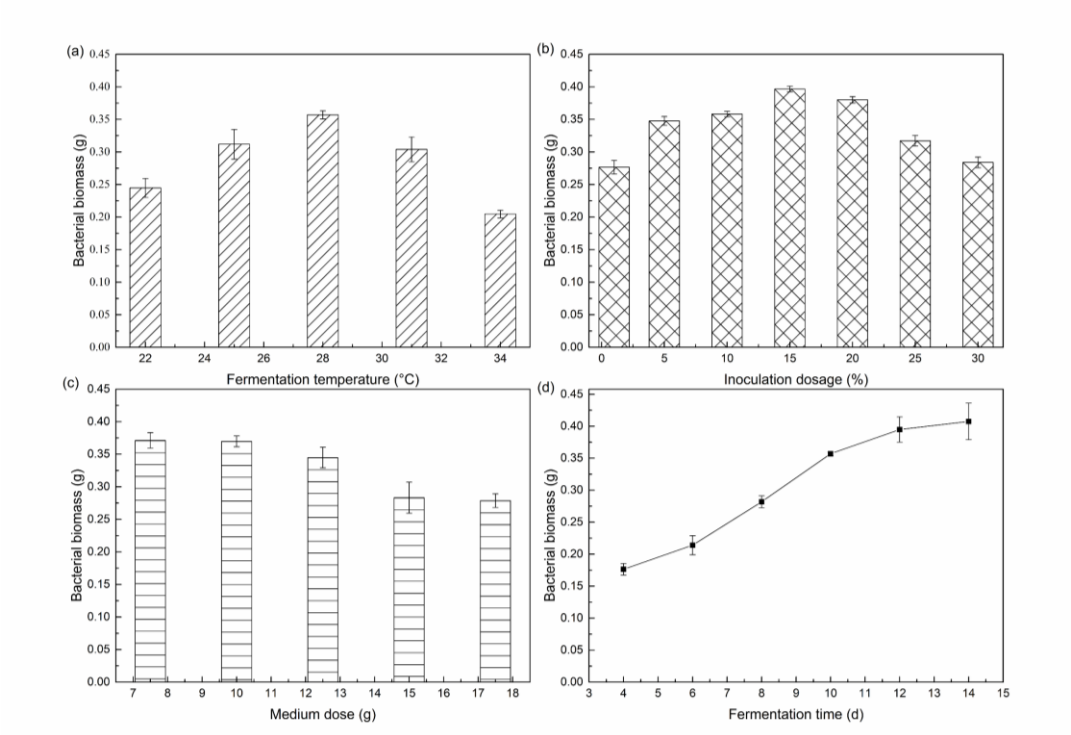

Figure 1. Effects of fermentation temperature **(a)**, inoculation dosage **(b)**, medium dose **(c)**, and fermentation time **(d)** on *Ganoderma lucidum* mycelial biomass.

Response surface optimisation of Ganoderma lucidum mycelial biomass

Building and fitting the regression model

The response surface design and experimental results for *G. lucidum* mycelial biomass are given in Table 2. The experimental data were fitted with linear, two-factor interaction, quadratic, and cubic models to obtain regression equations. A sequential model sum of squares, lack of fit tests, and model summary statistics were used to determine the availability of the models. The cubic model was proven to be aliased, and the quadratic model was suggested to be more suitable for further research due to significant additional terms ($p < 0.05$), the insignificant lack of fit ($p > 0.05$), and the maximum "adjusted R^2" and "predicted R^2" values.

The empirical relationship between the value of *G. lucidum* mycelial biomass and the value of the experimental levels was given by Design-Expert 8.0 software (Stat-Ease, Inc.), and is shown in Equation 5. This equation can predict the *G. lucidum* mycelial biomass as an equation in terms of coded factors:

$$Y = 0.39 + 0.017X_1 + 6.525\text{E} - 003X_2 + 0.053X_3 - 5.350\text{E} - 003\,X_1X_2 - 0.012\,X_1X_3 + 0.012\,X_2X_3 - 0.041\,{X_1}^2 - 0.064\,{X_2}^2 - 0.012\,{X_3}^2 \quad \text{(Eq. 5)}$$

where, Y = value of *G. lucidum* mycelial biomass, X_1 = coded value of inoculum dosage; X_2 = coded value of fermentation temperature, and X_3 = coded value of fermentation time.

ANOVA for the response surface quadratic model

The predicted values of *G. lucidum* mycelial biomass obtained using Eq. 1 are listed in Table 2. The model *F* (152.79) and *p* (< 0.0001, less than 0.05) value implied that the model was significant, and the lack of fit *F* (4.15) and *p* (0.1014, greater than 0.05) value implied that the lack of fit was not significant relative to the pure error. The regression was statistically significant based on the correlation coefficient evaluation (R^2 = 0.9884), which showed that it can be used to predict the *G. lucidum* mycelial biomass in the fermentation system (Şenol *et al.*, 2020). The model predicted R^2 value of 0.9367 was in reasonable agreement with the adjusted R^2 value of 0.9884, and it could explain 93.76% of the response value change. The significance test results of the regression coefficients showed that the inoculum dosage (X_1) and fermentation time (X_3) had extremely significant effects on the *G. lucidum* mycelial biomass ($p < 0.01$), and the fermentation temperature (X_2) had a significant effect on its mycelial biomass ($p < 0.05$). The order of the effect degree of the main factors on the *G. lucidum* mycelial biomass was fermentation time (X_3) > inoculum dosage (X_1) > fermentation temperature (X_2) based on the F values.

Response surface optimisation and interaction of technological parameters

The interaction contours and 3D response surface optimisation of technological parameters on *G. lucidum* mycelial biomass are given in Figure 2.

In the response surface graph of Figure 2a, the fermentation time (X_3) was at the centre point (12 d) level, and the interaction between the inoculum dosage (X_1) and fermentation temperature (X_2) on the *G. lucidum* mycelial biomass was not significant, which was consistent with the results of the ANOVA ($p > 0.05$). Its biomass was lower when the values of X_1 and X_2 were both low. This was because the lower fermentation temperature would inhibit certain enzyme activities in *G. lucidum* cells and reduce their metabolism, and a lower inoculum dosage would increase its growth adaptation period. *G. lucidum* mycelial biomass decreased when the values of X_1 and X_2 were both too high. This was because *G. lucidum* could quickly adapt to the medium, and grow rapidly on its surface when the inoculum dosage was too high, while its growth inside the medium was restricted (Zhu *et al.*, 2011). The metabolic enzymes in *G. lucidum* were inactivated when the fermentation temperature was too high, thereby reducing its biomass.

In the response surface graph of Figure 2b, the fermentation temperature (X_2) was at the centre point (28°C) level, and the interaction between the inoculum dosage (X_1) and fermentation time (X_3) on the *G. lucidum* mycelial biomass was significant, which was consistent with the results of the ANOVA ($p < 0.05$). Its biomass was lower when the values of X_1 and X_3 were both low. This was because the lower inoculum dosage would increase the adaptation period of *Ganoderma lucidum* growth, and a shorter fermentation time reduced the yield.

In the response surface graph of Figure 2c, the inoculum dosage (X_1) was at the centre point (15%), and the interaction between the fermentation temperature (X_2) and fermentation time (X_3) on the *G. lucidum* mycelial biomass was significant, which was consistent with the results of the ANOVA ($p < 0.05$).

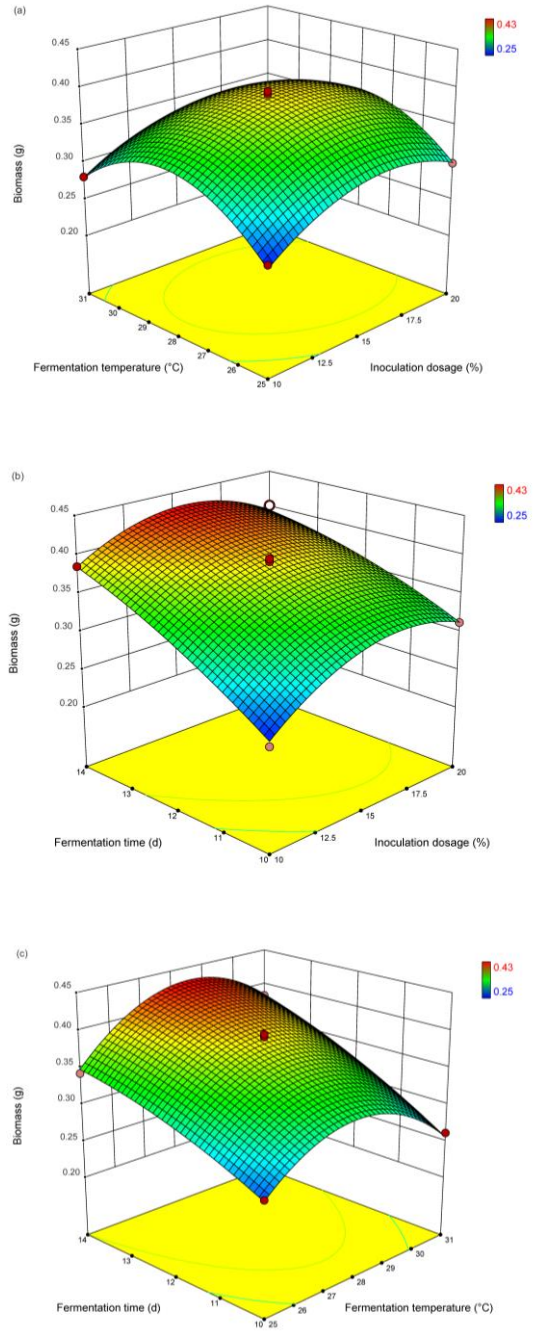

Figure 2. Response surface plot showing the effect and interaction of the three main factors on *Ganoderma lucidum* mycelial biomass: **(a)** effect of the inoculum dosage and fermentation temperature; **(b)** effect of the fermentation time and inoculum dosage; **(c)** effect of the fermentation time and fermentation temperature.

The extreme value of 0.4327 g of *G. lucidum* mycelial biomass in the fermentation system was predicted by the partial derivative of the multiple regression model and the analysis of the inverse matrix: the inoculum dosage (X_1) was 15.28%, the fermentation temperature (X_2) was 28.42°C, and the fermentation time (X_3) was 14 d. The verification experiment carried out at the optimum condition showed that an experimental value of 0.4205 g, and the relative error between it and the predicted value of 0.4327 g was 2.82%, thus confirming the adequacy of the model, and optimised technological parameters could improve the mycelial biomass of *G. lucidum* by SSF when compared with the single-factor experiments. The results provided a reference for the optimisation of technological parameters for producing *G. lucidum* by SSF from *P. notoginseng* residues.

Kinetics modelling of solid-state fermentation

Kinetics of Ganoderma lucidum growth

Ganoderma lucidum growth in *Panax notoginseng* residues during SSF can be described by the typical four-stage growth pattern (lag phase, logarithmic phase, stationary phase, and death phase). The lag period ranged from 0 to 4 d, the logarithmic period ranged from 5 to 13 d, and the stationary period ranged from 13 to 16 d. Its biomass reached the maximum value of 0.4408 g on the 15th d. A logistic equation (Eq. 1) was fitted to determine the model parameters X_m, X_0, and a (Figure 3a). The deviation between the predicted *G. lucidum* mycelial biomass and their experimental value occurred within 0 - 4 d, corresponding to the lag phase. The observed and predicted biomass values were significantly correlated (R^2 = 0.9754). Hence, the logistic equation (Qi and Wang, 1996; Gatto *et al.*, 1988) could verify the experimental data.

The statistical parameter values showed that the model was valid, and adequately described the experimental results.

The kinetics equation of *G. lucidum* growth during SSF based on the values of model parameters is given in Eqs. 6 and 7:

$$X = \frac{0.4433}{1+\left(\frac{0.4433}{0.0267}-1\right)e^{-0.4574t}} \quad \text{(Eq. 6)}$$

where, X = biomass of *G. lucidum* (g); and t = fermentation time (d).

$$\frac{dX}{dt} = 0.4574X\left(1-\frac{X}{0.4433}\right) \quad \text{(Eq. 7)}$$

The growth rate equation of *G. lucidum* was as follows, obtained by integrating Eqs. 6 and 7:

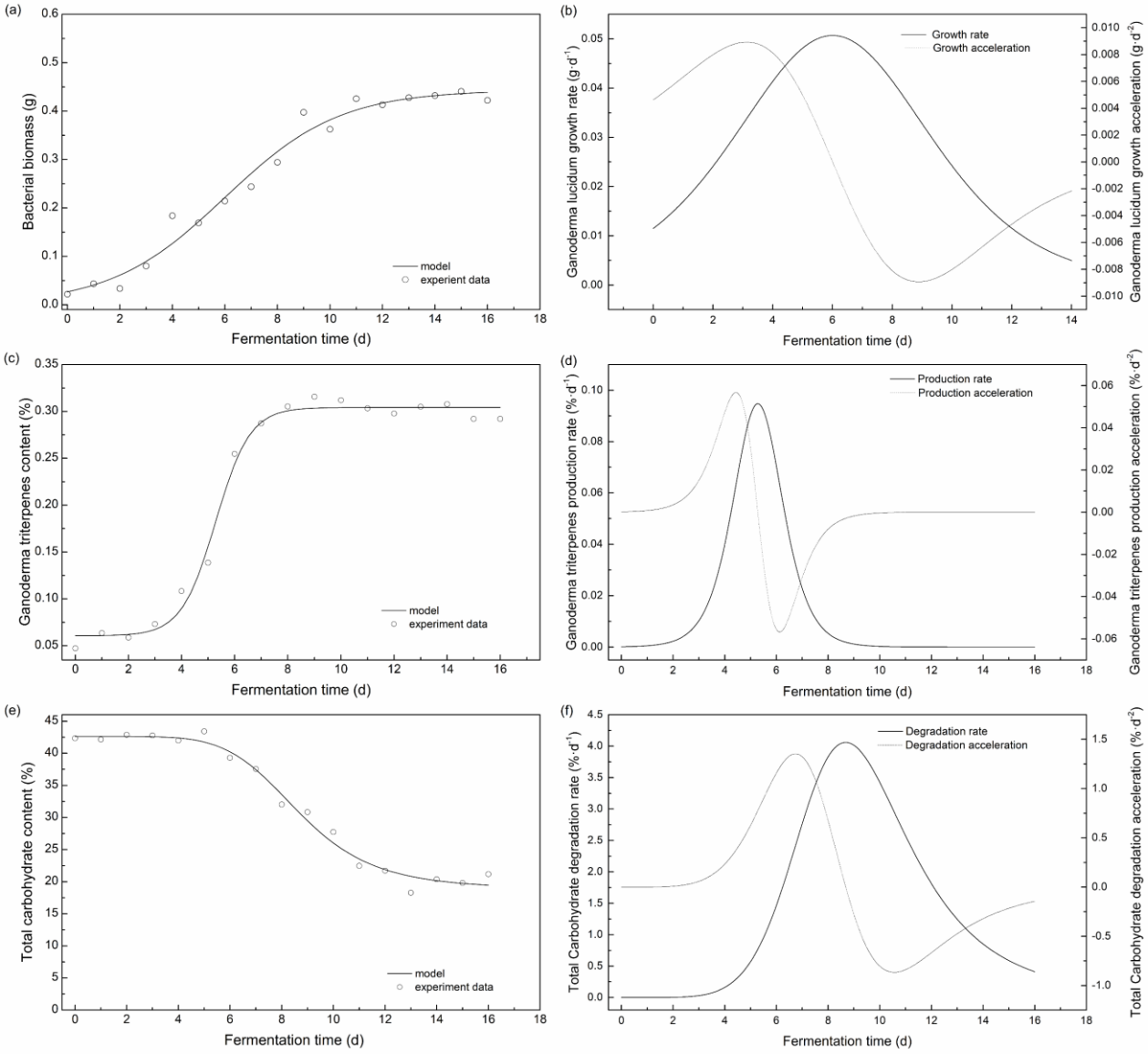

Figure 3. Kinetics of **(a)** *Ganoderma lucidum* growth, **(b)** growth rate and acceleration, **(c)** *Ganoderma* triterpenes production, **(d)** production rate and acceleration, **(e)** total sugar degradation, and **(f)** degradation rate and acceleration.

$$V_1 = \frac{dX}{dt} = \frac{0.2028}{1+15.603e^{-0.4574t}}\left(-\frac{1}{1+15.603e^{-0.4574t}}\right) \quad \text{(Eq. 8)}$$

where, V_1 = growth rate (g·d^{-1}).

The acceleration equation of *G. lucidum* growth was derived from Eq. 8:

$$a_1 = \frac{dV_x}{dt} = \frac{0.0928}{1+15.603e^{-0.4574t}}\left(1-\frac{1}{1+15.603e^{-0.4574t}}\right)\left(1-\frac{2}{1+15.603e^{-0.4574t}}\right) \quad \text{(Eq. 9)}$$

where, a_1 = growth acceleration (g·d^{-2}).

The maximum mycelial biomass of *G. lucidum* predicted by the growth kinetics model was 0.4362 g, which was close to the experimental value of 0.4408 g. The specific growth rate is an important parameter to control the maximum biomass, and to determine the induction or repression of *G. lucidum* synthesis. The maximum specific growth rate obtained based on the model was 0.4574 h^{-1}, which was close to the research of Lima-Pérez *et al.* (2019).

Figure 3b shows the growth rate of *G. lucidum* and its acceleration with time, which described the internal growth law of *G. lucidum* during fermentation. Its growth rate reached the maximum

value of 0.0507 g·d^{-1} on the 6th d of fermentation, and its growth acceleration reached the maximum and minimum values of 0.00893 and -0.00893 g·d^{-2} on the 3rd and 9th d of fermentation, respectively; that is, 0 - 3 d was its lag phase. After the 9th d, its growth rate gradually decreased to zero; therefore 3 - 9 d represented the rapid growth period of *G. lucidum*. Economic factors must be considered when determining the fermentation time in a project. When the production rate is low, the growth of products per unit volume is limited. If the fermentation time continues to be extended, the average production capacity will decrease, while the power consumption, equipment consumption, and other costs will increase, which will eventually lead to an increase in product costs. Therefore, from the perspective of the application, it is appropriate to control the fermentation time of *G. lucidum* within 9 d in the subsequent scale-up experiment, which was consistent with the research of Feng *et al.* (2014).

Product formation kinetics model

A Sigmoidal Boltzman's function (Eq. 3) was fitted to determine the model parameters B_1, B_2, t_0, and a (Figure 3c). The observed and predicted *G. lucidum* triterpene production values were significantly correlated (R^2 = 0.9897). Hence, a sigmoidal Boltzman's function (Hait *et al.*, 2002) could verify the experimental data. The statistical parameter values showed that the model was valid, and adequately described the experimental results.

The generation kinetics of *Ganoderma* triterpene during SSF based on the values of model parameters is given in Eq. 10.

$$y = 0.3041 - \frac{0.2434}{1+e^{\frac{t-5.2840}{0.6424}}} \quad \text{(Eq. 10)}$$

where, y = production of *Ganoderma* triterpenes (%); and t = fermentation time (d).

The production rate equation of *Ganoderma* triterpenes was as follows, which was obtained by deriving the variable t in Eq. 10:

$$V_2 = \frac{dy}{dt} = \frac{0.3789e^{\frac{t-5.2840}{0.6424}}}{(1+e^{\frac{t-5.2840}{0.6424}})^2} \quad \text{(Eq. 11)}$$

where, V_2 = *Ganoderma* triterpene production rate (%·d^{-1}).

The production acceleration equation of *Ganoderma* triterpene was obtained by deriving the variable t in Eq. 11:

$$a_2 = \frac{dv}{dt} = \frac{0.5898e^{(t-5.2840)/0.6424)} \times (1-e^{(t-5.2840)/0.6424)})}{(1+e^{(t\text{-}5.2840)/0.6424})^3} \quad \text{(Eq. 12)}$$

where, a_2 = *Ganoderma* triterpene production acceleration (%·d^{-2}).

Figure 3c shows that the production of *Ganoderma* triterpenes at 0 - 3 d was relatively low, increased rapidly at 3 - 7 d, and did not increase after 7 d. However, the mycelial biomass of *G. lucidum* was still increasing during this time (Figure 3a). The increasing trend of *Ganoderma* triterpene production during 0 - 7 d was consistent with that of the *G. lucidum* mycelial biomass, which was simultaneous, thus indicating that the synthesis of *Ganoderma* triterpenes was attributed to cell growth (Feng *et al.*, 2014). After 7 d, *Ganoderma* triterpenes no longer increased, which may be caused by the decrease in dissolved oxygen in the matrix and the autolysis of the mycelia (Zhao *et al.*, 2011). This result was consistent with the research of Yu *et al.* (2004) and Wang *et al.* (2011).

Figure 3d shows the production rate of *Ganoderma* triterpenes and their acceleration with time, which describes the internal production law of *Ganoderma* triterpenes during fermentation. The production rate of *Ganoderma* triterpenes reached a maximum value of 0.09472%·d^{-1} on the 5.3rd d of fermentation, and then gradually decreased to zero. Its production acceleration reached maximum and minimum values of 0.05675 and -0.05675%·d^{-2} on the 4.5th and 6.1st d of fermentation, respectively; that is, *Ganoderma* triterpenes were produced slowly. After 6.1 d of fermentation, the production rate gradually decreased to zero. The rapid production period of *Ganoderma* triterpenes ranged from the 4.5th to the 6.1st d. After 9 d of fermentation, the production rate of *Ganoderma* triterpenes was zero, and its production reached the maximum value of 0.31%, which can be observed in the production kinetics curve of *Ganoderma* triterpenes (Figure 3c).

After 9 d, the production rate of *Ganoderma* triterpenes was zero; that is, the production amount remained unchanged. At this time, the production of *Ganoderma* triterpenes reached the maximum

(0.31%), which can be observed in the kinetics of *Ganoderma* triterpene production (Figure 3c).

Therefore, from the perspective of the application, it is cost-effective to control the fermentation time of *G. lucidum* within 6 d when the scale-up experiment was carried out to obtain *Ganoderma* triterpenes. At this time, the product growth rate reached the maximum, which was consistent with the research of Feng *et al.* (2014).

Matrix consumption kinetics model

A four-parameter logistic equation (Culpepper, 2016) (Eq. 4) was fitted to determine the model parameters C, D_0, $t_{50\%}$, and k_0 (Figure 3e). The observed and predicted total carbohydrate values were significantly correlated (R^2 = 0.9826). Hence, the four-parameter logistic equation could verify the experimental data. The statistical parameter values showed that the model was valid, and adequately described the experimental results.

The matrix consumption kinetics of total carbohydrates based on the values of model parameters is given in Eq. 13:

$$R = 218.8378 + \frac{23.7737}{1+\left(\frac{t}{8.6864}\right)^{5.9337}} \quad \text{(Eq. 13)}$$

where, R = total carbohydrate content (%); and t = fermentation time (d).

The degradation rate equation of total carbohydrate was as follows, obtained by deriving the variable t in Eq. 14:

$$V_3 = \frac{d(C-R)}{dt} = \frac{16.2399\times\left(\frac{t}{8.6864}\right)^{5.9337}}{[1+\left(\frac{t}{8.6864}\right)^{5.9337}]^2} \quad \text{(Eq. 14)}$$

where, V_3 = total carbohydrate degradation rate (%·d^{-1}).

The degradation acceleration equation of total carbohydrate was obtained by deriving the variable t in Eq. 14:

$$a_3 = \frac{dV_3}{dt} = \frac{11.0935\times(\frac{t}{8.6864})^{4.9337}\cdot\left[1-\left(\frac{t}{8.6864}\right)^{5.9337}\right]}{[1+\left(\frac{t}{8.6864}\right)^{5.9337}]^3} \quad \text{(Eq. 15)}$$

where, a_3 = total carbohydrate degradation acceleration (%·d^{-2}).

Figure 3f shows the degradation rate of total carbohydrates and their acceleration with fermentation time. The degradation rate of total carbohydrate was very low, and remained almost unchanged from the beginning to the 3rd d of fermentation. This is because *G. lucidum* was in the adaptation stage, its consumption of total carbohydrates was minimal, and the metabolic enzymes secreted by *G. lucidum* (such as amylase, cellulose-degrading enzyme, and lignin-degrading enzyme) could convert starch, cellulose, and lignin in *P. notoginseng* residues into carbohydrates, thus resulting in a low total carbohydrate degradation rate in the medium. After 3rd d, *G. lucidum* gradually adapted to the medium, began to multiply, and increased the demand for nutrients. The degradation rate of total sugar gradually increased, reaching a maximum value of 4.0514%·d^{-1} on the 8.5th d of fermentation, and the production of *Ganoderma* triterpenes reached a maximum (Figure 3c). Its production acceleration reached the maximum and minimum values of 1.3532 and -0.8665%·d^{-2} on the 7th and 10.5th d of fermentation, respectively; that is, the degradation rate of total carbohydrate continually increased from the 3rd to the 7th d, gradually decreased from the 7th to the 10.5th d, and gradually stabilised after the 10.5th d. This was consistent with the change law of *G. lucidum* mycelial biomass and *Ganoderma* triterpene production (Figures 3a and 3c).

The relationship between the growth and enzyme secretion of *G. lucidum* and substrate degradation is very complex. Enzyme secretion is usually highest during the active growth period of biomass (Cairns *et al.*, 2019). We studied the changes in the CMC enzyme, amylase, and total sugar contents in the substrate with time during the fermentation of *G. lucidum*. It was found that the change in CMC enzyme activity was consistent with the substrate degradation rate; that is, when the CMC enzyme activity was the highest, the substrate consumption rate was the fastest (the degradation rate was 4.0514%·d^{-1}), which occurred on the 8.5th d of fermentation, thus indicating that the growth and metabolism of *G. lucidum* may be closely related to the CMC activity in the fermentation system with *P. notoginseng* residue as the substrate. Gomes *et al.* (2021) found that fungal growth may be related to the activity of the protease.

In summary, the fermentation time and inoculum dosage had a clear effect on the *G. lucidum* mycelial biomass. The predicted maximum biomass of *G. lucidum* was 0.4327 g under the optimal technical parameters, and these optimised parameters resulted in a significant increase in its mycelial biomass. The logistic equation, the Boltzmann

function, and the four-parameter logistic equation were, respectively, suitable for modelling the *G. lucidum* growth kinetics, the *Ganoderma* triterpene production kinetics, and the matrix consumption kinetics. These models can be used to predict the SSF process and provide a theoretical basis for the industrial production of *G. lucidum*. Meanwhile, the recycling of *P. notoginseng* residue can be realised.

Conclusion

Optimisation of *G. lucidum* mycelial biomass and kinetics modelling were performed in the present work. The BBD experimental method was used to optimise the technical parameters, and the results showed that the predicted maximum biomass of *G. lucidum* was 0.4327 g under the optimal technical parameters, and these optimised parameters resulted in a significant increase in its biomass. The logistic equation, the Boltzmann function, and the four-parameter logistic equation were, respectively, suitable for modelling the *G. lucidum* growth kinetics, the *Ganoderma* triterpene production kinetics, and the matrix consumption kinetics. Based on the kinetic models, the production rate of *Ganoderma* triterpenes reached a maximum value of $0.09472\%\cdot d^{-1}$ on the 5.3^{rd} d, and the production acceleration reached a minimum value of $-0.05675\%\cdot d^{-2}$ on the 6.1^{st} d. Therefore, it was cost-effective to control the fermentation time within 6 d to obtain *G. lucidum* triterpenes. The change in CMC enzyme activity was consistent with the substrate degradation rate, and *G. lucidum* growth and metabolism may be related to the CMC activity. These models can be used to predict the SSF process and provide a theoretical basis for the industrial production of *G. lucidum*.

Acknowledgement

The financial support was received from the Science and Technology Department of Sichuan Province of China (Project No.: 2021YFG0263) and Chengdu Science and Technology Bureau (Project No.: 2019-YF05-02457-SN).

References

Akihisa, T., Nakamura, Y., Tagata, M., Tokuda, H. and Kimura, Y. 2007. Anti-inflammatory and anti-tumor-promoting effects of triterpene acids and sterols from the fungus *Ganoderma lucidum*. Chemistry and Biodiversity 2(4): 224-231.

An, Q., Li, C. S., Yang, J., Chen, S. Y., Ma, K. Y., Wu, Z. Y., ... and Han, M. L. 2021. Evaluation of laccase production by two white-rot fungi using solid-state fermentation with different agricultural and forestry residues. BioResources 3(16): 5287-5300.

Berovic, M., Podgornik, B. B. and Gregori, A. 2022. Cultivation technologies for production of medicinal mushroom biomass - Review. International Journal of Medicinal Mushrooms 2(24): 1-22.

Boh, B., Berovic, M., Zhang, J. and Zhi-Bin, L. 2007 . *Ganoderma lucidum* and its pharmaceutically active compounds. Biotechnology Annual Review 13: 265-301.

Cairns, T. C., Zheng, X., Zheng, P., Sun, J. and Meyer, V. 2019. Moulding the mould: Understanding and reprogramming filamentous fungal growth and morphogenesis for next generation cell factories. Biotechnology for Biofuels 77(12).

Chen, H., Chen, L., Chen, M. and Qin, J. 2006. *Ganoderma lucidum* cultivation with herb residues and components analysis. Transactions of the Chinese Society of Agricultural Engineering 14(22): 167-170.

Chinese Pharmacopoeia. 2015. Pharmacopoeia of the People's Republic of China. China: China Medical Science Press.

Culpepper, S. A. 2016. Revisiting the 4-parameter item response model: Bayesian estimation and application. Psychometrika 4(81): 1142-1163.

Dan, X., Liu, W., Jack, H. W. and Ng, T. B. 2016. A ribonuclease isolated from wild *Ganoderma lucidum* suppressed autophagy and triggered apoptosis in colorectal cancer cells. Frontiers in Pharmacology 7: 217.

Fazenda, M. L., Harvey, L. M. and McNeil, B. 2010. Effects of dissolved oxygen on fungal morphology and process rheology during fed-batch processing of *Ganoderma lucidum*. Journal of Microbiology and Biotechnology 4(20): 844-851.

Feng, J., Zhang, J., Jia, W., Yang, Y., Liu, F. and Lin, C. 2014. An unstructured kinetic model for the improvement of triterpenes production by *Ganoderma lucidum* G0119 based on nitrogen source effect. Biotechnology and Bioprocess Engineering 4(19): 727-732.

Gandia, A., Brandhof, J., Appels, F. and Jones, M. P. 2021. Flexible Fungal materials: Shaping the future. Trends in Biotechnology 39(12): 1321-1331.

Gatto, M., Muratori, S. and Rinaldi, S. 1988. A functional interpretation of the logistic equation. Ecological Modelling 2(42): 155-159.

Gomes, A., Casciatori, F. P., Gomes, E., Nunes, C., Moretti, M. and Thomeo, J. C. 2021. Growth kinetics of *Myceliophthora thermophila* M.7·7 in solid-state cultivation. Journal of Applied Microbiology 130: 90-99.

Gu, K., Qin, J. and Che, H. 2005. New solid fermentation of 14 *Ganoderma* strains and the study on polysaccharose content of the fermentation product. Lishizhen Medicine and Materia Medica Research 4(16): 313-314.

Guan, J., Zhang, T., Cui, J. and Li, Y. 2008. Study on bacterial protein produced from cassava residue. Journal of Anhui Agricultural Sciences 22: 9556-9558.

Hait, S. K., Moulik, S. P. and Palepu, R. 2002. Refined method of assessment of parameters of micellization of surfactants and percolation of W/O microemulsions. Langmuir 7(18): 2471-2476.

Hariharan, S. and Nambisan, P. 2013 . Optimization of lignin peroxidase, manganese peroxidase, and Lac production from *Ganoderma lucidum* Under solid state fermentation of pineapple leaf. BioResources 1(8): 250-271.

Hsu, B., Lu, T. J., Chen, C. H., Wang, S. J. and Hwang, L. S. 2013. Biotransformation of ginsenoside Rd in the ginseng extraction residue by fermentation with Lingzhi (*Ganoderma lucidum*). Food Chemistry 4(141): 4186-4193.

Hu, H., Ahn, N., Yang, X., Lee, Y. and Kang, K. 2002. *Ganoderma lucidum* extract induces cell cycle arrest and apoptosis in MCF-7 human breast cancer cell. International Journal of Cancer 3(102): 250-253.

Huie, C. W. and Di, X. 2004. Chromatographic and electrophoretic methods for Lingzi pharmacologically active components. Journal of Chromatography B 812: 241-257.

Jang, S., Cho, S., Yoon, H., Jang, K., Song, C. and Kim, C. 2014. Hepatoprotective evaluation of *Ganoderma lucidum* pharmacopuncture: *In vivo* studies of ethanol-induced acute liver injury. Journal of Pharmacopuncture 3(17): 16-24.

Ko, H., Hung, C., Wang, J. and Lin, C. 2008 . Antiinflammatory triterpenoids and steroids from *Ganoderma lucidum* and *G. tsugae*. Phytochemistry 1(69): 234-239.

Lam, F. F. Y., Ko, I. W. M., Ng, E. S. K., ShanTam, L., Leung, P. C. and MingLi, E. K. 2008. Analgesic and anti-arthritic effects of Lingzi and San Miao San supplementation in a rat model of arthritis induced by Freund's complete adjuvant. Journal of Ethnopharmacology 1(120): 44-50.

Li, H., Zhong, Y., Li, S., Sun, K., Zhang, X., Yao, Y., ... and Chen, T. 2019. Isolation and purification of *Panax notoginseng* polysaccharide and its effect on proliferation of human periodontal ligament stem cells and mice osteoblasts *in vitro*. West China Journal of Pharmaceutical Sciences 5(34): 433-439.

Lima-Pérez, J., López-Pérez, M., Viniegra-González, G. and Loera, O. 2019. Solid-state fermentation of *Bacillus thuringiensis* var kurstaki HD-73 maintains higher biomass and spore yields as compared to submerged fermentation using the same media. Bioprocess and Biosystems Engineering 9(42): 1527-1535.

Liu, W., Xu, J., Jing, P., Yao, W., Gao, X. and Yu, L. L. 2010. Preparation of a hydroxypropyl *Ganoderma lucidum* polysaccharide and its physicochemical properties. Food Chemistry 4(122): 965-971.

Mahapatra, S. and Banerjee, D. 2013. Fungal exopolysaccharide: Production, composition and applications. Microbiology Insights 6: 1-16.

Mowsumi, F. R., Rahman, M. M., Rahaman, A. and Hossain, S. 2013. Preventive effect of *Ganoderma lucidum* on paracetamol-induced acute hepatotoxicity in rats. Journal of Scientific Research,3(5): 573-578.

Nie, S., Zhang, H., Li, W. and Xie, M. 2013. Current development of polysaccharides from *Ganoderma*: Isolation, structure, and bioactivities. Bioactive Carbohydrates and Dietary Fibre 1(1): 10-20.

Qi, Y. and Wang, S. 1996. Biochemical reaction kinetics and reactor. Beijing: Chemical Industry Press.

Şenol, H., Erşan, M. and Görgün, E. 2020 . Optimization of temperature and pretreatments for methane yield of hazelnut shells using the response surface methodology. Fuel 271: 117585.

Tang, Y., Zhang, W. and Zhong, J. 2009. Performance analyses of a pH-shift and DOT-shift integrated fed-batch fermentation process for the production of ganoderic acid and *Ganoderma* polysaccharides by medicinal mushroom *Ganoderma lucidum*. Bioresource Technology 100: 1852-1859.

Tsujikura, Y., Higuchi, T., Miyamoto, Y. and Sato, S. 1992. JP04304890 - Manufacture of ganoderic acid by fermentation of *Ganoderma lucidum*. Japan: Japanese Patent.

Wang, W., Shang, D. and Wen, L. 2006. Quantitative analysis of triterpenoid in the mycelia of *Ganoderma lucidum*. Edible Fungi of China 1(25): 30-32.

Wang, X., Zhao, Y., Liu, G. and Kuang, S. 2011 . Unstructured kinetic models for triterpene acids of *Ganoderma lucidum* in batch fermentation. Mycosystema 30(5): 767-773.

Yang, F., Hsieh, C. and Chen, H. 2004. Use of stillage grain from a rice-spirit distillery in the solid state fermentation of *Ganoderma lucidum*. Process Biochemistry 1(39): 21-26.

Yu, S., Zhang, J., Tang, Q., Shi, X., Liu, Y. and Yang, Y. 2004. Correlation between intracellular triterpenes from mycelia of *Ganoderma lucidum* in different growth stage and inhibition effect on tumor cells. Mycosystema 23: 548-554.

Yuan, M., Xiang, R., Peng, X., Yu, D., Shu, B., Deng, S., ... and Xu, Z. 2020. Research progress on production of functional feed by solid-state fermentation of traditional Chinese medicine residues. China Brewing 3(39): 17-20.

Zhao, R., Chen, Q. and He, Y. 2018. The effect of *Ganoderma lucidum* extract on immunological function and identify its anti-tumor immunostimulatory activity based on the biological network. Scientific Reports 1(8): 12680.

Zhao, Y., Liu, G., Zhu, C., Han, W. and Li, D. 2011. Effects of extracts from different phytomedicines on cell growth and intracellular triterpenoid formation of *Ganoderma lucidum* in submerged fermentation. Mycosystema 30(2): 249-254.

Zhu, Q., Xia, Y., Chen, A. and Xiong, X. 2011. Optimization of *Ganoderma lucidum*-*Astragalus* membranaceus polysaccharide solid fermentation condition by response surface analysis. China Biotechnology 12(31): 99-103.